A Quantitative Study of Potassium Channel Kinetics in Rat Skeletal Muscle from 1 to 37°C

KURT G. BEAM and P. LYNN DONALDSON

From the Department of Physiology and Biophysics, University of Iowa School of Medicine, Iowa City, Iowa 52242

ABSTRACT Potassium currents were measured using the three-microelectrode voltage-clamp technique in rat omohyoid muscle at temperatures from 1 to 37°C. The currents were fitted according to the Hodgkin-Huxley equations as modified for K currents in frog skeletal muscle (Adrian et al., 1970*a*). The equations provided an approximate description of the time course of activation, the voltage dependence of the time constant of activation (τ_n), and the voltage dependence of g_{K_∞}. At higher temperatures the relationship between g_{K_∞} and voltage was shifted in the hyperpolarizing direction. The effect of temperature on τ_n was much greater in the cold than in the warm: τ_n had a Q_{10} of nearly 6 at temperatures below 10°C, but a Q_{10} of only ~2 over the range of 30–38°C. The decreasing dependence of τ_n on temperature was gradual and the Arrhenius plot of τ_n revealed no obvious break-points. In addition to its quantitative effect on activation kinetics, temperature also had a qualitative effect. Near physiological temperatures (above ~25°C), the current was well described by n^4 kinetics. At intermediate temperatures (~15–25°C), the current was well described by n^4 kinetics, but only if the n^4 curve was translated rightward along the time axis (i.e., the current had a greater delay than could be accounted for by simple n^4 kinetics). At low temperatures (below ~15°C), n^4 kinetics provided only an approximate fit whether or not the theoretical curve was translated along the time axis. In particular, currents in the cold displayed an initial rapid phase of activation followed by a much slower one. Thus, low temperatures appear to reveal steps in the gating process which are kinetically "hidden" at higher temperatures. Taken together, the effects of temperature on potassium currents in rat skeletal muscle demonstrate that the behavior of potassium channels at physiological temperatures cannot be extrapolated, either quantitatively or qualitatively, from experiments carried out in the cold.

INTRODUCTION

Most quantitative studies of voltage-dependent ionic channels have been carried out using invertebrates and cold-blooded vertebrates. Only recently

Address reprint requests to Dr. Kurt G. Beam, Dept. of Physiology and Biophysics, University of Iowa, Iowa City, IA 52242.

J. GEN. PHYSIOL. © The Rockefeller University Press · 0022-1295/83/04/0485/38 $1.00 485
Volume 81 April 1983 485/512

have ionic currents in mammalian peripheral nerve and skeletal muscle been studied with voltage-clamp methods (Adrian and Marshall, 1977; Brismar, 1980; Chiu et al., 1979*b*; Duval and Léoty, 1978, 1980*a*, *b*; Pappone, 1980). For the most part, these studies have been carried out at temperatures considerably below the physiological range (e.g., 15–20°C). The reason for using low temperatures, particularly in the case of sodium channels, is that channel gating is slower in the cold and hence much easier to study.

In this paper we describe experiments designed to characterize the gating of potassium channels in mammalian skeletal muscle over a range of temperatures from near 0°C up to physiological. In mammalian skeletal muscle, K channels are important for determining the shape of action potential (Adrian and Marshall, 1976; Pappone, 1980), and the efflux of potassium ions through K channels may contribute to repetitive firing in certain muscle disease states (Adrian and Marshall, 1976). Pappone (1980) has presented a partial quantitative analysis of K currents in cut fibers of rat muscle, but her work and other studies of K channels in rat muscle (Duval and Léoty, 1978, 1980*a*, *b*) describe currents at subphysiological temperatures.

Given the importance of K channels to the electrophysiology of mammalian skeletal muscle, one goal of our work was to obtain a complete description of these channels in terms of the Hodgkin-Huxley (1952) equations and to compare the results of this analysis at several different temperatures. Ordinarily, the assumption is made that one can extrapolate a channel's function at physiological temperatures from its behavior at colder temperatures. This extrapolation requires that two conditions be met. The first is that the channel behave in the cold in a manner that is qualitatively similar to its behavior in the warm. The second is that a linear relationship hold between the logarithm of time constants and temperature. Our results demonstrate that in the case of K channels in mammalian muscle neither condition is met.

A second reason for examining the effects of temperature is that temperature provides a useful probe of a channel's kinetic states and of its physicochemical environment. For example, abrupt changes in the Arrhenius plot of one or more properties of chemically and voltage-gated ionic channels in avian and mammalian muscle tissue have been interpreted to mean that the membrane lipids of these cells undergo a phase transition (Dreyer et al., 1976; Lass and Fischbach, 1976; Chiu et al., 1979*a*). Although we have found that the Arrhenius plot of the rate of K channel activation is nonlinear, the results suggest that either such a phase transition does not occur in the membrane of rat skeletal muscle, or if it does occur, it does not affect K channel function. Additionally, it appears that cooling reveals kinetic steps in potassium channel gating that are not evident at higher temperatures. A preliminary account of some of the results reported here has appeared (Beam, 1981).

METHODS

The omohyoid, a fast-twitch skeletal muscle (Müntener et al., 1980) from male Sprague-Dawley rats weighing 400–500 g, was used in all experiments. This muscle has the advantage that it is thin, which aids survival in vitro. More importantly, approximately two-thirds of its fibers do not run all the way from the hyoid bone to

the scapula, but instead terminate on a central tendon that runs at roughly a right angle to the long axis of the muscle. This abrupt, well-defined termination of fibers is readily accessible, which makes this an ideal preparation for the three-microelectrode technique (see below). At all times during the dissection the muscle was superfused with oxygenated solution A (see Table I). After removal of surface connective tissue in the region of the tendon, the muscle was mounted in a small experimental dish (5 ml), in which it was supported from below by a piece of nylon mesh. The dish was mounted on the stage of a compound microscope and continuously perfused at 5 ml/min with oxygenated solution B. The mesh aided oxygenation by allowing the solution to bathe thoroughly both the top and bottom of the muscle. The composition of solution B is given in Table I; it contained sucrose to abolish contractions, tetrodotoxin (TTX) to block sodium currents, elevated Ca to aid the electrode sealing process, and impermeant anions to eliminate the large contribution of Cl to the resting membrane conductance (Camerino and Bryant, 1976; Palade and Barchi, 1977). The temperature of the muscle bath was electronically controlled. A small thermistor, located close to the site of the microelectrode penetrations, was used to monitor the temperature continuously.

TABLE I
SOLUTIONS

	Na	K	Ca	Mg	Sucrose	Anion
	mM	*mM*	*mM*	*mM*	*mM*	*mM*
A	151	5	2	1	0	157 (Cl)
B	151	5	10	1	350–400	146 (methylsulfate) 27 (acetate)

Both solutions contain $HEPES^-$ (5), $HEPES^{+-}$ (5), and glucose (0.2%). Solution B contains TTX (1 μM).

Ionic currents were measured with the three-microelectrode method (Adrian et al., 1970*a*). In this method, voltage-measuring microelectrodes V_1 and V_2 are introduced at distances l and $2 \times l$, respectively, from the tendon end of a fiber, and a third, current-passing microelectrode is introduced a distance l' from the V_2 microelectrode. The voltage from V_1 is fed back as the error signal to the voltage-clamp amplifier. The membrane current per unit fiber length is measured as proportional to ΔV, the difference between V_2 and V_1:

$$i_m = 2\Delta V/3l^2 r_i,$$

where r_i is the longitudinal resistance per unit fiber length. In the experiments reported here, the distance l was 140–300 μm; l' was 40–75 μm. The signals from the V_1 and V_2 microelectrodes were led to FET-input amplifiers mounted as close to these electrodes as possible. Voltages were measured differentially with respect to the bath potential, which was monitored by an Ag-AgCl/agar electrode attached to an FET follower. A separate Ag-AgCl/agar electrode served as the current ground. Microelectrodes were fabricated from thin-walled aluminosilicate capillary tubing and filled with 3 M KCl (for voltage measurement, resistance 3–6 MΩ) or 2 M K-citrate (for current passing, resistance 5–10 MΩ). The voltage electrodes were painted with Q-dope (G.C. Electronics, Rockford, IL) to within 100 μm of the tip in order to decrease capacitance to bath ground. This procedure produced electrodes that had voltage responses sufficiently fast (time constant of <50 μs) that additional electronic compensation for electrode capacitance was not used.

After amplification and electronic filtering, the signals ΔV, V_1 (the controlled voltage), and I were sampled by an A/D converter and stored in the memory of a PDP 11/03 computer (Digital Equipment Corp., Marlboro, MA). Depending on the time course of the response in question, the data were recorded at a rate of 1, 4, or 10 kHz.

To check the quality of microelectrode penetrations, the resting cable properties of the fiber were computed at the start of each voltage-clamp run. The potential at V_1 was stepped from −90 to −135 mV for 100 ms and then repolarized to −90 mV. The current elicited by the repolarizing step was used to calculate (cf. Eqs. 1–3 and 5,

TABLE II

CABLE PROPERTIES OF THE RAT'S OMOHYOID MUSCLE

Muscle	T	λ	r_i	C_m	V_K
	°C	μm	MΩ/cm	μF/cm²	mV
64-11-2	6.7	636	11.1	8.4	−67
71-7-1	7.2	525	19.6	11.5	−70
30-3-25	8.7	594	10.7	6.0	−80
37-6-4	10.4	374	18.3	9.3	−75
33-1-1	15.1	806	7.6	7.1	−80
64-7-3	14.4	547	7.6	11.6	−72
64-8-2	14.6	550	14.1	4.7	−72
37-6-2	16.2	377	15.3	10.4	−80
63-2-5	14.6	596	4.8	6.1	−80
65-6-2	15.0	637	7.7	13.5	−68
33-1-6	20.5	870	5.6	8.1	−90
64-13-2	20.6	499	11.5	6.6	−82
62-5-2	21.0	493	5.5	14.6	−75
48-3-2	23.0	348	16.5	7.7	−90
37-6-9	21.6	367	21.0	4.7	−70
30-3-46	27.2	593	6.7	7.8	−80
33-1-16	31.4	724	4.9	8.7	−90
30-3-56	37.3	583	5.7	8.8	−77
74-1-8	38.5	870	4.2	10.0	−90
74-1-4	30.9	697	6.9	8.7	−90
64-15-3	29.8	740	6.5	11.4	−85
65-7-2	30.3	623	5.5	12.0	−75

Schneider and Chandler, 1976, for computational details): r_i, λ, the fiber's space constant, and c_m, the capacitance per unit length. The latter quantity was converted to C_m, the specific membrane capacity, by using a calculated fiber diameter. Values for λ, r_i, and C_m for representative fibers are summarized in Table II. The fiber diameter, d, was calculated according to:

$$d = 2\sqrt{\rho/\pi r_i},$$

where ρ, the internal resistivity, was assumed to be 220 Ωcm at 20°C, with a Q_{10} of 1.37 (Hodgkin and Nakajima, 1972). In addition to its use in computing C_m, the calculated diameter was also used to calculate the fiber area from which current densities were determined.

Test currents were elicited by depolarizing command pulses superimposed on the holding potential, −90 mV. The command pulses were rounded with a single time constant of 50–300 μs. Test currents were corrected for linear components of capacitative and ionic leakage currents by digital subtraction of an appropriately scaled control current, elicited by depolarizing the fiber from −90 to −60 mV.

Two kinds of pulse protocols were used. In the standard protocol the sequence was: three control pulses, test pulses to voltages in odd multiples of 10 mV (−50, −30, −10 . . . V_{max}), three control pulses, and test pulses to potentials in even multiples of 10 mV (−60, −40, −20 . . . V_{max} − 10). The individual pulses were delivered 2 or, more commonly, 5 s apart. A similar sequence was used for tail current experiments except that each of the individual test pulses was replaced by a paired pulse in which a step to a constant-amplitude conditioning pulse was followed by a step to a variable potential ranging from −100 to −30 mV.

RESULTS

Hodgkin-Huxley Analysis

Potassium currents recorded at physiological temperature from a rat omohyoid muscle are illustrated in Fig. 1. The currents qualitatively resemble potassium currents that others have measured in muscles and axons of invertebrates and cold-blooded vertebrates. To facilitate a more quantitative comparison, we

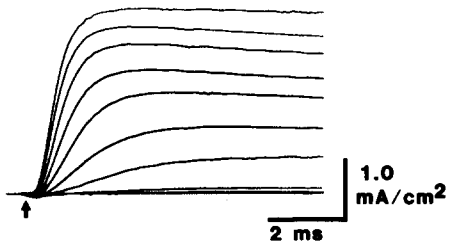

FIGURE 1. Potassium currents in a rat omohyoid muscle fiber at physiological temperature. Currents were elicited by test pulses at 10-mV intervals from −60 to +30 mV. The upward arrow indicates the onset of the test pulses. Temperature, 38°C. Muscle 74-1, run 8: $l, l' = 140, 60$ μm; $r_i = 4.2$ MΩ/cm; $\lambda = 870$ μm; $C = 10$ μF/cm^2.

have followed the standard procedure for quantifying K currents in a new preparation, which is to fit them to the Hodgkin-Huxley (HH) equations (Hodgkin and Huxley, 1952). The following section summarizes this HH analysis, including a description of the *I-V* behavior of open channels, the steady-state conductance vs. voltage relationship, and the voltage dependence of activation kinetics.

The *I-V* behavior of open K channels was determined in experiments like the one illustrated in Fig. 2. The currents in Fig. 2A were obtained by depolarizing the fiber to +10 mV and then repolarizing it to test levels varying from −30 to −100 mV (tail currents). As the test level was varied from −30 to −100 mV, the tail currents became less outward, reversed direction, and

became inward. The horizontal ticks indicate the magnitude of the tail currents 750 μs after the onset of the pulses, which repolarized the fiber from +10 mV to the test level. Under the assumption that channels neither opened nor closed during this 750-μs interval, the current indicated by the ticks

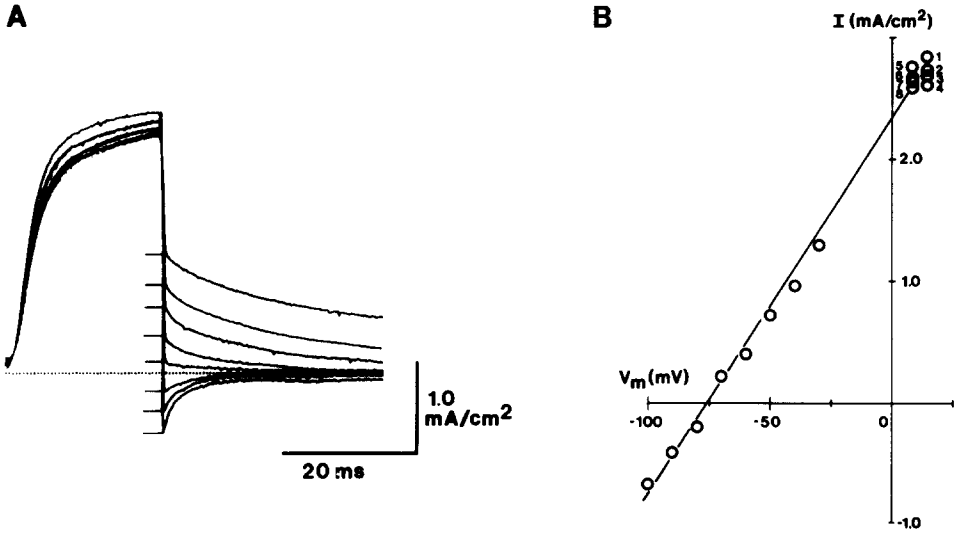

FIGURE 2. Potassium tail currents and the resulting instantaneous current-voltage relationship. Eight individual current traces are shown superimposed in A. Each of the individual eight traces was elicited by a two-step pulse: a 25-ms conditioning step to +10 mV followed by a variable test step to potentials ranging from −100 (largest inward tail current) to −30 mV (largest outward tail current), at 10-mV intervals. The ticks give the amplitude of the current 0.75 ms after the voltage was stepped from the conditioning level to the test level. These amplitudes are plotted as a function of test level in B. The points plotted in the upper right-hand portion of this frame represent the current at the end of the individual conditioning steps during each of the conditioning-step, test-step pulse pairs. The points plotted in a vertical column to the right of +10 mV are from pulse pairs 1–4, those to the left are from pulse pairs 5–8. The current was largest during the first conditioning pulse and diminished with successive pulses. The pulse pairs were separated by 2 s, except that the 4th and 5th pulse pairs were separated by an 8-s interval, during which three control pulses were administered. Note that the amplitude of the conditioning pulse current recovered considerably in the 8-s interval between the 4th and 5th pulse pairs. Temperature, 14.5°C. Muscle 64-7: l, l' = 140, 50 μm; r_i = 7.6 MΩ/cm; λ = 547 μm; C = 11.6 μF/cm^2.

represents the instantaneous current-voltage relationship of an approximately constant number of open channels. This relationship is illustrated in Fig. 2B for the fiber in Fig. 2A. Over the range of potentials from −100 to +10 mV, the current-voltage relationship is linear, which indicates that open potassium channels in rat omohyoid muscle behave ohmically, similar to K channels in frog muscle (Adrian et al., 1970*a*).

V_K, the equilibrium potential for potassium current flow, was −75 mV for the fiber illustrated in Fig. 2. Table II summarizes the value of V_K measured for a number of fibers over a range of temperatures. In general, V_K was less negative (more depolarized) at lower temperatures. The experimental methodology may have contributed to this effect because it was not possible to measure V_K with an identical pulse protocol at all temperatures. In particular, it was necessary to vary the duration of the conditioning pulse from 10 ms at temperatures above ~20°C to 25 ms for temperatures from 10 to 20°C and to 100 ms for temperatures below 10°C. These durations were chosen in an attempt to maximally activate channels without causing inactivation or potassium accumulation. At the highest temperatures, inward tail currents could not be reliably measured because they decayed too rapidly to be well resolved by the voltage clamp. Thus, above 25°C, V_K was obtained by linearly extrapolating the instantaneous *I-V* relationship determined at potentials of −80 mV and above where the voltage clamp was able to resolve tail current kinetics.

A linear instantaneous current-voltage relationship, together with the assumption that open channels have only a single conductance level (cf. Begenisich and Stevens, 1975), implies that the potassium conductance given by

$$g_K = I_K/(V - V_K) \tag{1}$$

is a measure of the relative number of open channels. The quasi-steady-state voltage dependence of channel-opening probability was obtained by substituting the peak outward current at different potentials into Eq. 1. Fig. 3 illustrates the normalized peak g_K vs. voltage relationship for one fiber at 7°C, a second fiber at 21°C, and a third at 30°C. The data points show an orderly dependence on temperature. As temperature is increased, the conductance vs. voltage relationship shifts to the left. A similar effect was observed when peak g_K vs. voltage data were obtained from single fibers at several different temperatures.

The smooth curves in Fig. 3 were calculated according to the relationships:

$$g_K/g_{K,max} = n_\infty{}^4 \tag{2}$$

where

$$n_\infty = \alpha_n/(\beta_n + \alpha_n), \tag{3}$$

$$\alpha_n = \bar{\alpha}_n(V - \bar{V}_n)/(1 - \exp[(\bar{V}_n - V)/k_{\alpha_n}]), \tag{4}$$

$$\beta_n = \bar{\beta}_n \exp[(\bar{V}_n - V)/k_{\beta_n}]. \tag{5}$$

The values used for the parameters $\bar{\alpha}_n$, $\bar{V}_n$, k_{α_n}, $\bar{\beta}_n$, and k_{β_n} are given in Table III.

Obtaining reliable conductance-voltage data was complicated by the presence of ordinary and cumulative inactivation of the current. The term ordinary inactivation designates the slow decline of outward current during a

maintained depolarization. The test pulses used in our experiments were usually short enough to prevent ordinary inactivation, although at higher temperatures a small amount was present. (For example, the largest outward current in Fig. 10B reaches a maximum and then declines ~5%.) Cumulative inactivation is manifest as a successive decrement of peak current in response

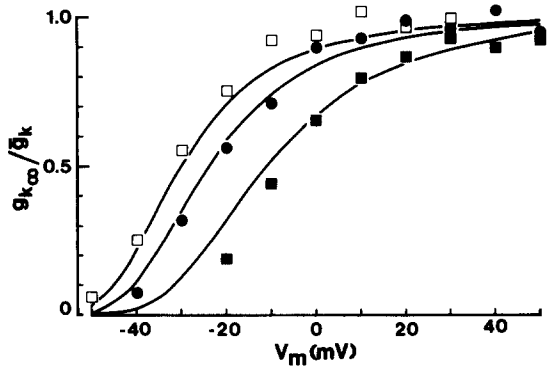

FIGURE 3. Normalized plot of g_K vs. voltage at 7 (filled squares), 21 (filled circles), and 30°C (open squares). Points were determined from measured currents according to Eq. 1. Smooth curves represent n_∞^4, where n_∞ was calculated according to Eqs. 3–5. For details on the fitting procedure see text; the parameters of fit appear in Table III.

TABLE III

VALUES OF CONSTANTS DERIVED BY FITTING EQS. 2–7 AND 9 TO POTASSIUM CURRENTS IN RAT OMOHYOID MUSCLE

Muscle	Temperature	$\bar{\alpha}_n$	$\bar{\beta}_n$
64-11	7	0.00178	0.0204
64-8	15	0.00634	0.0304
64-13	21	0.0134	0.0669
64-15	30	0.0332	0.102

The smooth curves in Figs. 3 and 5 all used $\bar{V}_n = -40$ mV, $k_{\alpha n} = 7$ mV, $k_{\beta n} = 40$ mV. The values of $\bar{\alpha}_n$ ($ms^{-1}mV^{-1}$) and $\bar{\beta}_n$ (ms^{-1}) are given above. (Note: to avoid crowding the illustration, the data of g_K vs. potential for the fiber at 15°C have been omitted from Fig. 3.)

to the repeated application of identical test pulses. Such cumulative inactivation is present in Fig. 2, where the current during the conditioning pulse becomes smaller with successive pulses. Cumulative inactivation typically occurred even for test pulses sufficiently short that ordinary inactivation was not apparent (e.g., Fig. 2). It appeared to be greater in fibers with poor electrode penetrations and in fibers impaled for a long time. It was not, however, simply a consequence of a continual voltage-independent fiber rundown since this cumulative inactivation was smaller the longer the interval was between test pulses. Thus, Fig. 2B illustrates that the cumulative inacti-

vation that occurred for test pulses applied every 2 s is largely reversed by the 8-s interval between the fourth and fifth test pulses.

Because significant cumulative inactivation of g_K would obviously distort the shape of the steady-state conductance-voltage relationship, several steps were taken to minimize this source of error. First, conductance data were usually obtained at a single temperature from freshly impaled fibers (rather than from single fibers at several temperatures). Second, data were obtained in a sequence designed to detect whether significant cumulative depression occurred. Specifically, (*a*) outward currents were measured with the standard pulse protocol (see Methods); (*b*) V_K was measured using the pulse protocol for tail currents; (*c*) the standard pulse protocol was repeated except that all the test pulses had the amplitude V_{max} of the largest test pulse. Data were rejected if peak outward current during this last sequence declined >15%. Fig. 4 summarizes conductance-voltage data, obtained from a number of fibers

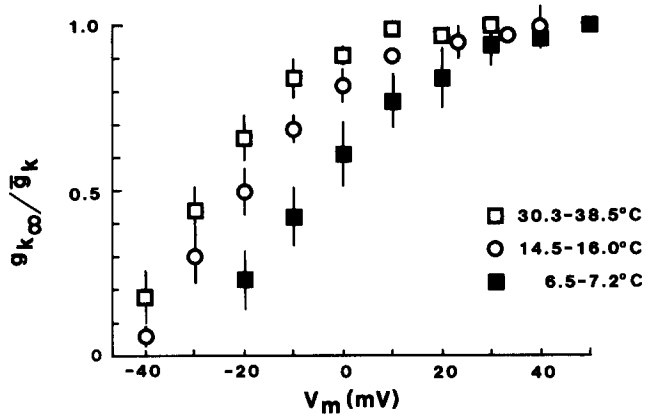

FIGURE 4. The effect of temperature on g_K vs. voltage. Each point represents the mean conductance for three to five fibers (see Table IV). Before averaging, the $g_K(V)$ values for a given fiber were normalized relative to the conductance at +50 mV, except for temperatures above 30°C, where the normalization was based on the conductance at +30 mV. Table IV gives the average values of $\bar{g}_K$ in these fibers as a function of temperature. Note that for the sake of clarity the points at +20 and +30 mV for $T \cong 15$°C are displaced to the right. The error bars represent ±1 SD.

under the experimental conditions described above. These pooled data confirm the behavior shown by the three individual fibers illustrated in Fig. 3: as temperature is increased, the g_K vs. voltage curve shifts in the hyperpolarizing direction. In addition to shifting the conductance-voltage relationship, raising the temperature increases $\bar{g}_K$, the maximal potassium conductance (Table IV). The increase of $\bar{g}_K$ with temperature is consistent with the hypothesis that (*a*) during outward currents elicited by strong depolarizations, the number of channels open at the peak of current is relatively independent of temperature, and (*b*) the temperature dependence of an open channel's

conductance is close to that of free diffusion. Thus, increasing the temperature from an average value of 6.8 to 32.4°C caused $\bar{g}_K$ to increase from 12.7 to 30.9 mS/cm^2, which corresponds to a Q_{10} of 1.42. By way of comparison, the increase in the equivalent conductance of a K ion in water between 0 and 25°C corresponds to a Q_{10} of 1.28 (Weast, 1971).

The time course of K channel activation was quantified by fitting the measured currents to n^4 kinetics:

$$I_K(t) = \bar{g}_K(V - V_K)n(t)^4; \quad (6)$$

$$n(t) = n_\infty + (n_o - n_\infty)e^{-t/\tau_n}. \quad (7)$$

At the holding potential (−90 mV), steady-state activation of K channels is expected to be zero. Thus, for currents activated by depolarizing steps from this holding potential, $n_o = 0$ and Eqs. 6 and 7 reduce to

$$I_K(t) = I_{K_\infty}[1 - \exp(-t/\tau_n)]^4, \quad (8)$$

where I_{K_∞} is the peak outward current, and τ_n is the voltage-dependent time constant of the hypothetical n parameter described by Eq. 7. Eq. 8 was fitted

TABLE IV
EFFECT OF TEMPERATURE ON $\bar{g}_K$

Temperature	$\bar{g}_K$	C_m
	mS/cm^2	$\mu F/cm^2$
6.5–7.2 ($N = 3$)	12.7±8.3	10.8±2.2
14.5–16.0 ($N = 5$)	22.1±5.8	9.3±3.7
20.6–23.0 ($N = 4$)	21.6±10.8	8.4±4.3
30.3–38.5 ($N = 4$)	30.9±11.5	10.5±1.5

All values are expressed as mean ±SD. The g_K vs. voltage relationships for the fibers at $T \cong 7$°C, $T \cong 15$°C, and $T > 30$°C are illustrated in Fig. 4.

to individual currents by adjusting the values of τ_n and I_{K_∞}. As will be discussed in detail later, for certain temperatures there were systematic deviations between the measured potassium currents and the predictions of Eq. 8. Although these deviations indicate that n^4 kinetics cannot be taken as a literal description of K channel gating in the omohyoid, they do not strongly influence the fitted value of τ_n and hence are unimportant for the present analysis.

Fig. 5 illustrates the voltage dependence of τ_n^{-1} for four representative fibers at 7, 15, 21, and 30°C (data points are to the right of the vertical broken line). The smooth curves represent τ_n^{-1} calculated according to the relationship

$$\tau_n^{-1} = \alpha_n + \beta_n, \quad (9)$$

where α_n and β_n are given by Eqs. 4 and 5. The theoretical curves in Fig. 5 were obtained by adjusting the values of $\bar{\alpha}_n$ and $\bar{\beta}_n$, with the constraint of fitting not only the measured values of τ_n^{-1} but also the g_K vs. voltage points measured in the same fibers (Fig. 3). The values of $\bar{\alpha}_n$ and $\bar{\beta}_n$ are given in

Table III. At ~20°C these values are close to those reported by Pappone (1980) for rat extensor digitorum longus and sternomastoid muscles at the same temperature. Additionally, both in Pappone's work and in ours, the parameters $\bar{V}_n$, k_{α_n}, and k_{β_n} have the same values used by Adrian et al. (1970*a*) to describe potassium currents in frog skeletal muscle.

The rate of channel deactivation was quantified by fitting tail currents according to Eqs. 6 and 7. For tail currents at sufficiently hyperpolarized test potentials, $n_\infty = 0$ and Eqs. 6 and 7 predict simple exponential decay

$$I_K = I_o \exp(-4t/\tau_n),$$

with time constant $\tau_n/4$ and amplitude I_o, the value of the current immediately after the step from the conditioning to the test potential. At less hyperpolarized

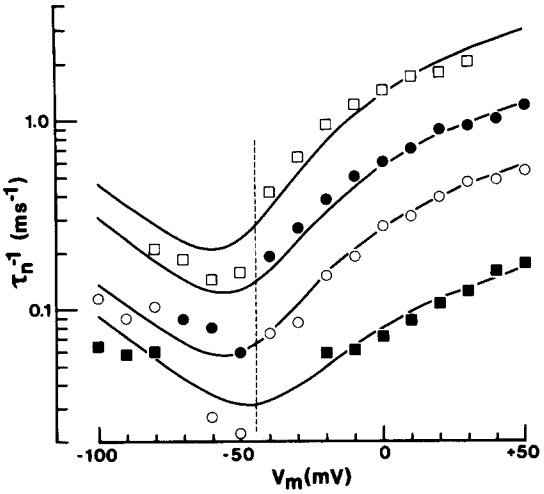

FIGURE 5. Dependence of τ_n^{-1} on voltage at 7 (filled squares), 15 (open circles), 21 (filled circles), and 30°C (open squares). For membrane potentials of −40 mV and above, τ_n was calculated by fitting Eq. 8 to current records like those in Fig. 1; for potentials of −50 mV and below τ_n was determined by fitting n^4 kinetics (Eqs. 6–7) to tail current records, like those in Fig. 2. The smooth curves were calculated according to Eqs. 4, 5, and 9. The parameters used to calculate these curves appear in Table III.

potentials, $n_\infty > 0$ and Eqs. 6 and 7 predict a tail current that decays as the sum of four exponentials having time constants of τ_n, $\tau_n/2$, $\tau_n/3$, and $\tau_n/4$, and amplitudes that are a function of n_o and n_∞. At many potentials a direct estimate of n_∞ is difficult since g_{K_∞} can be negligible even though n_∞ is appreciable. For example, when $n_\infty = 0.33$, one-third its maximal value, g_K is only ~1% of its maximal value. Additionally, the goodness of kinetic fit does not change dramatically with the value chosen for n_∞: in Fig. 6A a tail current is fitted according to Eqs. 6 and 7 with n_∞ arbitrarily chosen to be 0.33; in Fig. 6B the same current is fitted with $n_\infty = 0$. The fit with $n_\infty = 0.33$ appears to be only slightly better than that with $n_\infty = 0$. Although the goodness of fit was

not much different, the value determined for τ_n was. Changing n_∞ from 0 (Fig. 6B) to 0.33 (Fig. 6A) caused the value of τ_n to decrease from 107 to 68 ms.

In the absence of objective criteria for estimating n_∞, the method adopted for fitting tail current decay was to first fit Eqs. 2–5 and 9 to τ_n and g_K, measured in an individual fiber for test pulses in the range that activated

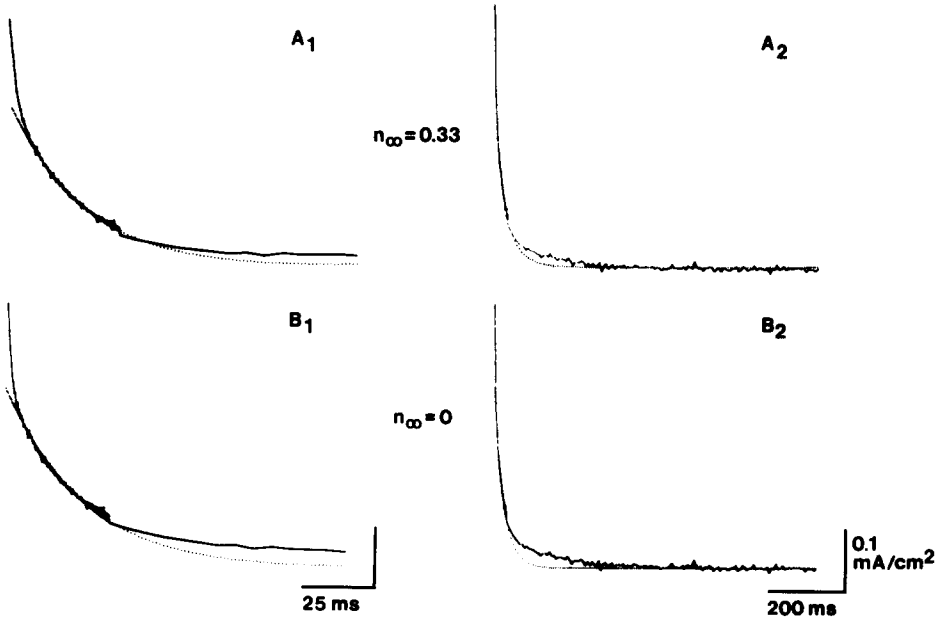

FIGURE 6. Tail current at −50 mV compared with n^4 kinetics (A) and simple exponential decay (B). In both A and B the same measured current (continuous curve) is compared with a theoretical curve on a fast (1) and slow (2) time base. A_1, A_2: n^4 kinetics (Eqs. 6 and 7) with $n_o = 1$; $n_\infty = 0.33$; $\tau_n = 68$ ms. B_1, B_2: single exponential with time constant of 26.8 ms, which corresponds to a τ_n of 107.2 ms. Theoretical curves represent visual best fits. Pulse protocol: 25-ms depolarization from −90 to +10 mV, followed by a step to −50 mV. Only that portion of the current following the onset of the step to −50 mV is shown, which occurred at the left of the illustrated trace. Temperature, 14.3°C. Muscle 52-2: l, $l' = 140$, 50 μm; $r_i = 13.5$ MΩ/cm; $\lambda = 606$ μm; $C = 7.5$ μF/cm^2.

significant outward currents ($V \geq -40$); Eq. 3 was then used to calculate n_∞ for potentials below this range. The calculated values for n_∞ were substituted into Eqs. 6 and 7, leaving only two free parameters, τ_n and I_o, which were adjusted for optimal fit of individual tail currents. This procedure relies on the ability of a specific model to fit the measured g_K vs. voltage data, but the measurement of τ_n depends on this model in any case.

The points to the left of the vertical broken line in Fig. 5 represent τ_n^{-1}, where τ_n was determined by the method just described for fibers at four different temperatures. The values of τ_n^{-1} generally fall below the theoretical curve, which successfully describes τ_n^{-1} for channel activation at the same

temperature. The magnitude of this discrepancy appeared to be larger at potentials just subthreshold for the activation of outward current than at more hyperpolarized potentials. The disagreement between predicted and measured τ_n for tail currents did not appear to be a consequence of an inaccurate estimation of n_∞. At depolarized potentials (−30 mV, for example), it was possible to directly determine n_∞ and to estimate τ_n for both activation and tail current decay. The value derived from tail currents was consistently slower than the value for activation.

To summarize the results of the HH analysis, the gating of K channels in the rat omohyoid appears to be similar to that in frog skeletal muscle. Thus, using the same parameters (Table III) descriptive of frog muscle (Adrian et al., 1970*a*), the HH equations give a good account of the steady-state and kinetic properties of activation and of the effect of voltage on these processes. The same equations give a much less satisfactory account of channel deactivation kinetics measured in tail current experiments. One of the discrepancies is the too-slow decay of tail currents. In addition, the HH theory gives an incomplete account of tail current time course. A consistent observation for tail currents at $V > -80$ was the presence of a small component of decay too slow to be fit by simple exponential (Fig. 6B) or n^4 (Fig. 6A) kinetics.

Temperature Dependence of the Rate of K Channel Activation

To examine in detail the effect of temperature on the rate of activation, currents in response to an identical test pulse were obtained from single fibers over a range of temperatures. A depolarization to +10 mV was chosen because it produced K currents whose activation kinetics could be accurately measured at temperatures from 1 to 37°C. In some experiments the muscle was gradually warmed; in others it was gradually cooled. In either case, the rate of change was ~1°C/min and currents were recorded at ~1° intervals. Fig. 7 shows a set of superimposed currents obtained from a single fiber at temperatures ranging from 8.7 (bottom trace) to 32.2°C (top trace). The illustrated traces represent currents at ~3° intervals. With increasing temperature the currents became larger and activated more rapidly. (The increase in size is a consequence both of the increase in $\bar{g}_K$ and the hyperpolarizing shift in the potential dependence of g_K; cf. Fig. 4.)

Qualitatively, the data in Fig. 7 show that a 3° change in temperature has a greater effect on activation kinetics in the cold than in the warm. The effect of temperature was quantified in terms of the τ_n obtained by fitting activation of the currents to Eq. 8. The Arrhenius plot in Fig. 8 summarizes the effect of temperature on τ_n in five fibers from three rats. Fig. 8 corroborates the qualitative impression given by the currents in Fig. 7: activation kinetics depend much more strongly on temperature in the cold than in the warm. At low temperatures the Q_{10} is nearly 6, whereas at high temperatures it drops to ~2. The decreased temperature dependence of τ_n could have been an artifact if the voltage clamp had been unable to resolve the rapidly changing currents elicited by test pulses to +10 mV at the higher temperatures. Such an artifact is unlikely because the same decreased temperature dependence is seen for

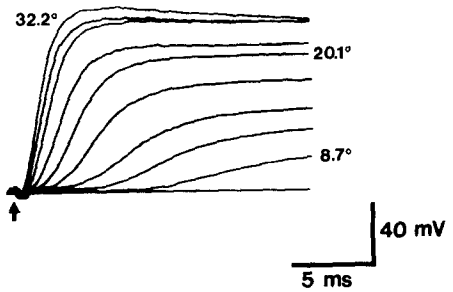

FIGURE 7. The effect of temperature on the rate of potassium current activation in rat skeletal muscle. The traces are superimposed currents from a single fiber, elicited by a test pulse to +10 mV (onset indicated by upward arrow). The currents were obtained at temperatures of 8.7, 11.5, 13.9, 17, 20.1, 22.9, 26.3, 29.1, and 32.2°C (lowest to highest trace). Currents from muscle 30-3: l, l' = 210, 70 μm; r_i = 10.2 MΩ/cm at 8.7 and decreased to 5.7 MΩ/cm at 32.2°C. At these two temperature extremes λ was 629 and 599 μm, respectively. Based upon an assumed specific resistivity (see Methods) and the measured cable properties, the computed fiber diameter remained fairly constant: 62 μm at 8.7°C, 57 μm at 32.2°C. Based on this computed diameter, 1 mV corresponds to 7.5 and 15.0 μA/cm^2 at 8.7 and 32.2°C, respectively.

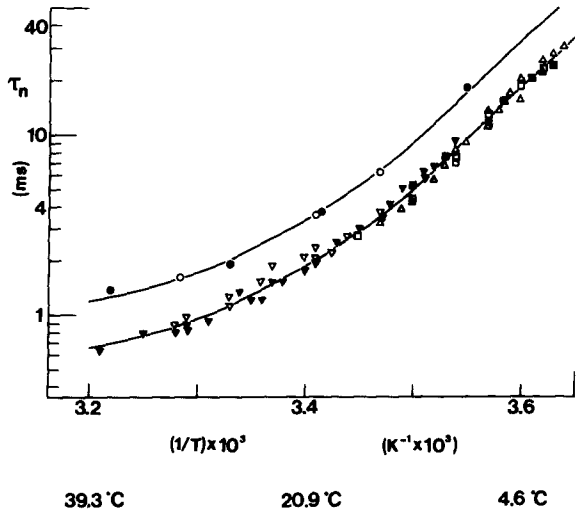

FIGURE 8. Arrhenius plot of τ_n. τ_n was determined by fitting n^4 (Eq. 8) to current records like those in Fig. 7. The circles (both open and filled) represent τ_n for currents elicited by a −20-mV test pulse; all the other symbols are for a +10-mV test pulse. The smooth curve was drawn by eye through the data points at +10 mV and shifted vertically upwards for comparison with the data points at −20 mV. The various symbols represent τ_n from different muscles and fibers: □, 18-1 (muscle fiber), down (direction of temperature change); ■, 18-2, up; △, 30-2, down; ▼, ●, 30-3, up; ○, ▽, 33-1, up.

test pulses to −20 mV, where activation is much slower (Fig. 8, circles: −20 mV; other symbols: +10 mV). Another possible explanation for the curved shape of the Arrhenius plot of τ_n, and for the decreased temperature dependence in the warm, is that n^4 kinetics do not provide an adequate method of characterizing K currents. However, other methods of characterizing the currents yield similar results. For example, the theoretical fits can be improved by the inclusion of a delay term (see below), but even with this third free parameter the Arrhenius plot of τ_n has the same general shape as illustrated in Fig. 8. Moreover, a less model-dependent characterization of channel kinetics can be obtained by fitting a single exponential to tail currents. Fig. 9 illustrates, as a function of potential, time constants from fibers at 7, 14, 21, and 30°C. Increasing the temperature from 14 to 21°C had a smaller effect on these time constants than increasing the temperature from 7 to 14°C; the effect of increasing temperature from 21 to 30°C was smaller still.

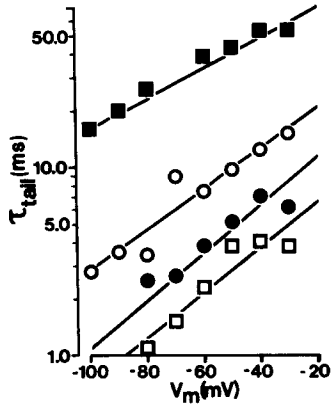

FIGURE 9. Voltage and temperature dependence of tail current time constant. Time constants are from single exponential fits, as in Fig. 6B. Solid lines are least-squares regressions. Filled squares: muscle 71-6, 7.2°C; open circles: muscle 64-7, 14.4°C; filled circles: muscle 64-13, 20.6°C; open squares: muscle 64-15, 29.9°C.

Qualitative Effects of Temperature on Activation Kinetics

In the course of analyzing activation kinetics it was noticed that these kinetics were qualitatively altered as a function of temperature. Fig. 10A illustrates a family of K currents obtained from a muscle fiber at 7°C, and Fig. 10B shows a family of currents from a fiber at 30°C. It can be seen that the time course of the currents is qualitatively dissimilar at the two temperatures. In particular, at 30°C the curvature of the rising phase of current is comparable at the "foot" and "shoulder," whereas at 7°C the curvature of the foot is much sharper than that of the shoulder. Besides demonstrating these kinetic differences, the currents at the two temperatures also demonstrate the leftward shift (Figs. 3 and 4) in the threshold voltage for activation of outward currents. At

30°C (Fig. 10B), the first trace exhibiting appreciable outward current was for a voltage step to −40 mV, whereas at 7°C (Fig. 10A), the first appreciable outward current was not activated until −30 mV.

As a method of characterizing the qualitative effects of temperature on activation kinetics, measured currents were compared with the predictions of Eq. 8 modified to include a delay term:

$$I_K(t + t_d) = I_K(\infty)[1 - \exp(-t/\tau_n)]^4. \quad (10)$$

Eq. 10 contains three free parameters: the steady-state current $I_K(\infty)$, the time constant τ_n, and the "delay" t_d, which slides the calculated curve to the right. For $t_d = 0$ the kinetics will be termed "n^4"; for $t_d > 0$ the kinetics will be termed "n^4 with delay."

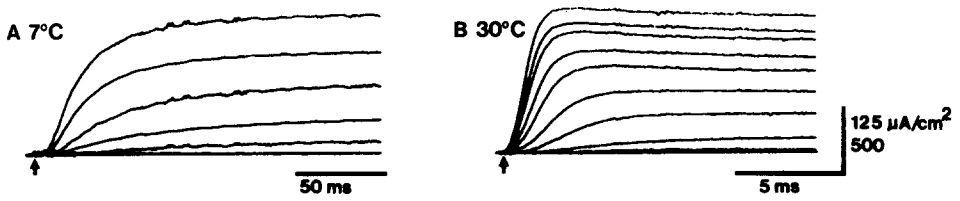

FIGURE 10. Potassium currents in rat omohyoid muscle fibers at 7°C (A) and 30°C (B). Currents were elicited by test pulses at +10-mV intervals, from −60 to +10 mV (A), or from −60 to +30 mV (B). Upward arrows indicate the time of onset of test pulses. Current calibration is 125 μA/cm² in A and 500 μA/cm² in B. Currents at 7°C are from muscle 18-2, run 5: l, l' = 280, 112 μm; r_i = 12.2 MΩ/cm; λ = 596 μm; C = 6.6 μF/cm². Currents at 30°C are from muscle 64-15, run 3: l, l' = 140, 50 μm; r_i = 6.5 MΩ/cm; λ = 740 μm; C = 11.4 μF/cm².

Fig. 11 examines the ability of simple n^4 kinetics to describe currents at +10 mV, the same test potential used in the experiment illustrated in Fig. 7. At 30°C (Fig. 11A), n^4 kinetics accurately describe the measured current except for the droop caused by inactivation. At 21°C (Fig. 11B), the measured current is not adequately fit with n^4 kinetics: at early times the theoretical curve rises faster than the measured current, whereas at later times it rises more slowly. Making τ_n shorter reduced the discrepancy at later times, but increased it at earlier times. Lengthening τ_n had the opposite effect. Although it is not shown, it was possible to achieve a very satisfactory fit of the current in Fig. 11B by the inclusion of a nonzero t_d in Eq. 10. One possible explanation for the necessity of including a delay to describe the current at 21 but not at 30°C, is that the current at the higher temperature was too fast to be well resolved by the voltage clamp. This explanation is ruled out by the observation that currents at −30 mV, where activation is considerably slower, showed the same behavior as those at +10 mV. Thus, even with this smaller depolarization it was found that simple n^4 kinetics adequately described the current at 30 (Fig. 12A) but not at 21°C (Fig. 12B$_1$). Fig. 12B$_2$ shows that n^4 kinetics-with-delay were able to well describe the current at 21°C.

By comparison with the currents at 21 and 30°C, the current at 10°C (Fig.

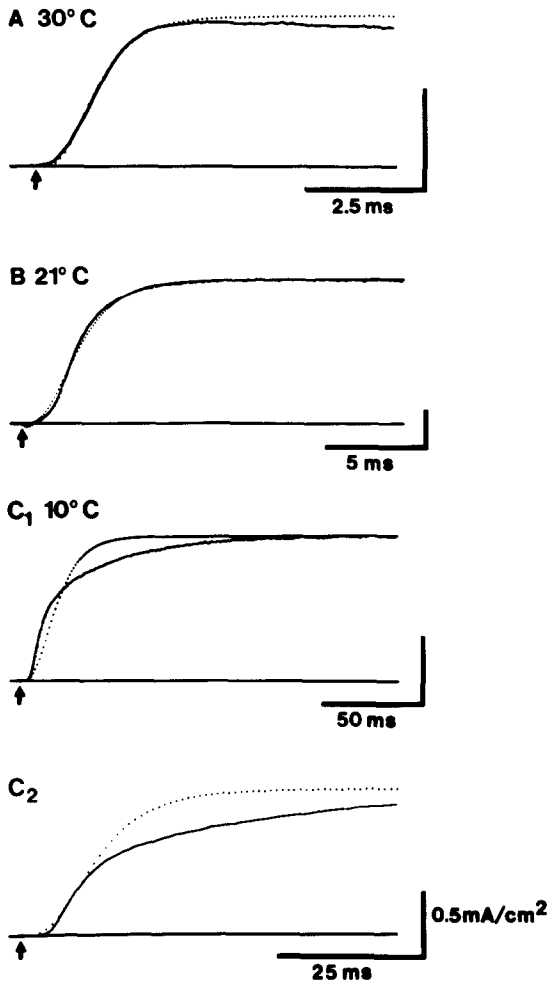

FIGURE 11. The effect of temperature on the ability of n^4 kinetics to fit potassium currents at +10 mV. Upward arrows indicate pulse onset. The broken lines, which represent visual best fits, were calculated according to Eq. 10 with zero delay ($t_d = 0$) and with $\tau_n = 0.62$ (A), 1.43 (B), 6.6 (C_1), and 9.3 ms (C_2). By including a nonzero delay in Eq. 10 it was possible to achieve a good fit of the trace in B: $t_d = 0.52$ ms, $\tau_n = 1.17$ ms. Note that the current at 30°C shows some inactivation. Trace A is from muscle 64-15, run 3 (cable properties given in legend to Fig. 10). Trace B is from muscle 64-13, run 2: l, $l' = 140$, 50 μm; $r_i = 11.5$ MΩ/cm; $\lambda = 499$ μm; $C = 6.6$ μF/cm^2. Trace C_1, C_2 is from muscle 76-3, run 3: l, $l' = 140$, 56 μm; $r_i = 10.5$ MΩ/cm; $\lambda = 545$ μm; $C = 11.9$ μF/cm^2.

11C_1) is not well described by n^4 kinetics. In particular, after an initial rising phase, which could be approximately fit with n^4 kinetics (Fig. 11C_2), the current at 10°C showed a second, slower phase of increase. Even with the inclusion of a nonzero delay term in Eq. 10 it was not possible to achieve a satisfactory fit of this current.

The currents illustrated in Figs. 11 and 12 are representative of the kinetic patterns observed at different temperatures. Although it is not possible to provide precise temperature limits over which a particular kinetic pattern was invariably observed, the following provides a reasonable summary of kinetic pattern as a function of temperature. Near physiological temperatures (roughly, >25°C), the measured currents are well described by simple n^4 kinetics with zero delay. At intermediate temperatures (~15–25°C), the currents are well described by n^4 kinetics only if a delay is included in Eq. 10. In the cold (roughly <15°C), the measured currents cannot be fit by n^4 kinetics whether or not a delay is included in Eq. 10.

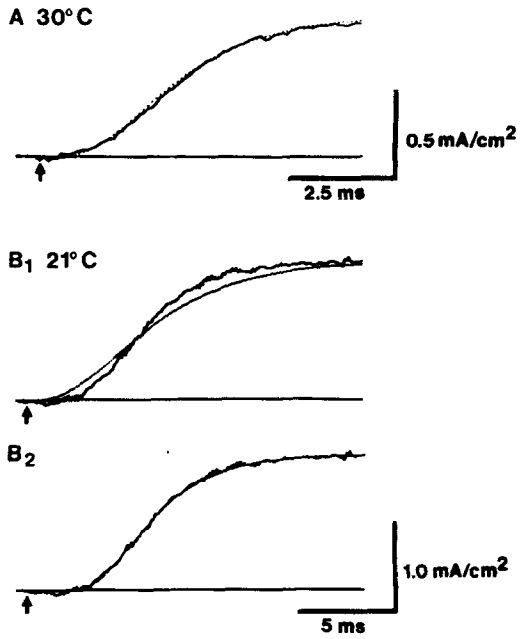

FIGURE 12. Fits of n^4 kinetics to K currents at −30 mV at two different temperatures. Upward arrows indicate pulse onset. The broken lines were calculated according to Eq. 10 with $t_d = 0$ and $\tau_n = 1.56$ (A) and 3.58 ms (B_1). In B_2 the theoretical curve used $\tau_d = 1.9$ ms and $\tau_n = 2.5$ ms. The trace in A is from muscle 64-15 (cable properties are given in the legend to Fig. 10). The trace in B_1, B_2 is from muscle 64-13 (cable properties are given in the legend to Fig. 11).

DISCUSSION

Three major observations are presented in this paper. First, there does not appear to be any profound quantitative difference between K channel gating in rat omohyoid muscle and frog twitch skeletal muscle. Second, changing temperature affects both the rate and steady-state voltage dependence of K activation in such a way that the physiological function of K channels at normal body temperature cannot be extrapolated from measurements made

in the cold. Third, cooling produces qualitative changes in activation kinetics which suggest that low temperatures reveal kinetic transitions in gating not apparent at higher temperatures.

The Hodgkin-Huxley (1952) equations provide a fair description of potassium channel gating in rat skeletal muscle. Thus, the time course of activation (Figs. 11 and 12), the voltage dependence of steady-state activation (Fig. 3), and the voltage dependence of the rate of activation (Fig. 5) can be approximated by Eqs. 2–9. In fitting these equations to the data, only the values of $\bar{\alpha}_n$ and $\bar{\beta}_n$ were varied: the values of k_{α_n}, k_{β_n}, and $\bar{V}_n$ were held fixed at the values descriptive of K currents in frog muscle (Adrian et al., 1970*a*) and used in Pappone's (1980) description of K currents in rat extensor digitorum longus and sternomastoid muscles. The resulting values for $\bar{\alpha}_n$ and $\bar{\beta}_n$ (0.0134 $ms^{-1}mV^{-1}$ and 0.0669 ms^{-1}, respectively) at 21°C are similar to those of Pappone (0.0132 $ms^{-1}mV^{-1}$ and 0.0556 ms^{-1}) at 20°C. In comparing the results of the two studies, two methodological differences should be pointed out. First, in our experiments the extracellular calcium concentration was 10 mM instead of 2 mM. Based on results from frog muscle (Costantin, 1968), the increased calcium should have shifted $\bar{V}_n$ from the −40-mV value we used to −33 mV. In some instances we did compute our theoretical curves with $\bar{V}_n$ = −33 mV instead of −40 mV, but the fits were somewhat less satisfactory. Moreover, the resulting values for $\bar{\alpha}_n$ and $\bar{\beta}_n$ were little affected by this change in $\bar{V}_n$. Second, Pappone's values of τ_n were derived from fits using n^4 kinetics with delay (i.e., Eq. 10), since the currents could not be accurately fit without this delay. In this regard, Pappone's results are entirely consistent with those of the present study. Nonetheless, we have chosen to present values derived from simple n^4 kinetics (Eq. 8) because (*a*) simple n^4 fits have only two free parameters compared with three for n^4-with-delay; (*b*) at low temperatures the fit provided by n^4-with-delay is not much better than that provided by simple n^4; and (*c*) the magnitude and voltage dependence of τ_n obtained with n^4-with-delay fits are not significantly different than those from simple n^4.

Temperature has two important quantitative effects that make it difficult to extrapolate K channel function at physiological temperatures from measurements made in the cold. These are the nonlinearity of the Arrhenius plot of τ_n and the shift in the g_K vs. voltage relationship. This shift is ~20 mV in the hyperpolarizing direction for an increase in temperature from ~7 to 37°C. In the Hodgkin-Huxley formalism, the shift in g_K means that the temperature dependence of $\bar{\alpha}_n$ is greater than that of $\bar{\beta}_n$. Put another way, raising the temperature appears to increase the voltage-independent free energy difference, which tends to drive channels from the closed to the open state. One alternative to a direct effect of temperature on channel gating is to suppose that the shape of the steady-state activation curve is influenced both by the voltage dependence of channel opening and by a voltage-dependent blocking reaction. An example of such a blocking reaction is the voltage-dependent proton block of sodium channels proposed by Woodhull (1973). If changing the temperature affected the extent of such a reaction, it would alter the potential dependence of the measured g_K. However, the observed linearity of

the instantaneous *I-V* relationship (Fig. 2) argues that a voltage-dependent blocking reaction does not significantly influence measured g_K, and hence argues against such a mechanism for the temperature-induced shift. A mechanism that does appear consistent with the data is the supposition that temperature alters the ionic affinity of charged groups on the surface of the membrane. For example, increasing proton concentration by one pH unit causes a 20-mV depolarizing shift of g_K in frog skeletal muscle (Blatz, 1981). If this were the reaction affected by temperature in the omohyoid, then a 10-fold drop in K_a would be necessary to account for the observed shift of g_K for a 30° increase in temperature.

Although the Arrhenius plot of τ_n deviates from a straight line, it nonetheless does not show the obvious sharp discontinuities of slope known as break-points. In particular, it shows no break-point at 6°C as described in rabbit nerve for τ_h, the time constant of sodium channel inactivation (Chiu et al., 1979*a*). Chiu et al. ascribed the break-point in rabbit nerve to a phase transition in membrane phospholipids. The absence of a break-point in the kinetics of potassium channels in mammalian muscle therefore raises a number of interesting possibilities. One is that a lipid phase transition does occur in muscle, but that the gating of potassium channels is relatively insensitive to the state of the surrounding lipid. It should be noted, however, that in invertebrate axons, small lipid-soluble molecules affect the kinetics of both potassium and sodium channels (Bean et al., 1981; Haydon and Kimura, 1981). Another possibility is that mammalian muscle differs significantly from mammalian myelinated nerve in that lipids in muscle do not undergo a phase transition at 6°C.

Interestingly, effects of temperature on K channel activation similar to those we have found in the omohyoid have been described for another preparation. By using hypertonic glycerol as "antifreeze," Kukita (1982) has measured K currents in squid giant axon at temperatures from +5 to −15°C. Over this range, the Arrhenius plot of the rate of K channel activation lacks obvious break-points and shows a gradual curvature such that the Q_{10} decreases as temperature is increased.

Voltage-Clamp Delays

As temperature is increased and K channel gating becomes more rapid, the kinetics of the measured currents will be contaminated to an increasing degree by imperfections in the spatial and temporal control of potential. Quantifying the effect of such imperfections is difficult, but the following estimate suggests that they are relatively unimportant except for strong depolarizations at the highest temperatures. The potential at the V_1 microelectrode can be taken as representative of imperfections in temporal control: in good fibers this potential settled to 90% of its final value in ~150 μs. An estimate of spatial imperfection of control can be obtained by treating the fiber as a one-dimensional cable whose termination at the tendon does not allow the escape of current. For the case in which the V_1 electrode is located 140 μm from the end of a fiber with a 700-μm length constant, a step in potential at V_1 will

produce a change in potential at the end of the fiber that reaches the 90% level within 0.04 τ_m, where τ_m is the membrane time constant (Waltman, 1966). For the high-frequency currents involved in producing a rapid change of voltage, this time constant corresponds to the product of surface resistance and capacitance. Taking the former to be on the order of 1 $k\Omega cm^2$ and the latter to be 2 $\mu F/cm^2$ (cf. Duval and Léoty, 1978; Pappone, 1980), one estimates that the potential at the end of the fiber lags that at V_1 by ~80 μs. (Note that the average spatial delay between V_1 and the fiber end will be less than this value.) Taken together, then, the temporal and spatial delays total ~200 μs.

A precise statement about the kinetic consequences of a 200-μs delay is difficult since it depends on knowing the reaction scheme for K channel gating. Nevertheless, it is clear that at most potentials and temperatures a delay of ~200 μs is short compared with the measured current transients. A variety of other considerations also make it seem unlikely that voltage-clamp delays have significantly contaminated the kinetics of the K currents we have measured at most temperatures and potentials. One of these is the quantitative agreement between the K currents we have measured with the three-microelectrode clamp at 20°C and the currents measured by Pappone (1980) using the vaseline-gap technique. Since clamp delays should have been negligible with the latter method, this agreement suggests that the three-microelectrode method is adequate to measure currents at temperatures up to at least 20°C. An argument that the three-microelectrode method is also able to resolve currents at 30°C is the similarity of the voltage dependence of τ_n at 30° with that of τ_n at 21° (Fig. 5): if the rate of channel opening at 30° had approached the rate at which the clamp was able to change potential, the rate of activation deduced from the measured currents would have been slower than the actual rate and therefore would have appeared to be less voltage dependent. One might also worry that clamp delays are responsible for the decreased temperature dependence of τ_n at high temperatures (Fig. 8). As already described in the Results section, however, the parallel temperature dependence of τ_n (−20 mV) and τ_n (+10 mV) argues against this notion.

It also seems unlikely that voltage-clamp delays are responsible for the qualitative effects of temperature on activation kinetics illustrated in Figs. 10–12. The slow phase of activation at low temperatures (Figs. 11C_1 and C_2) takes place on a time scale of tens of milliseconds, i.e., about two orders of magnitude more slowly than the time required for the settling of potential. In addition, settling delays cannot explain the observation that simple n^4 kinetics describe currents near physiological temperatures, whereas n^4-with-delay kinetics are required to describe currents at intermediate temperatures. First, this effect was observed not only for strongly depolarizing test pulses but also for weakly depolarizing ones. In the latter case it is clear that the time required for potential to settle is brief compared with the rate of activation (e.g., −30 mV; Fig. 12). Moreover, if the finite speed of the clamp were responsible for the necessity of including a delay term in order to fit currents at ~20°C (Fig. 11B), then for currents at 30° this same delay would be present and would in fact be proportionately larger in comparison with τ_n.

The values determined for C_m at the end of omohyoid muscle fibers (8.99 ± 2.68 $\mu F/cm^2$ in Table II) are somewhat larger than might be expected for mammalian fast-twitch muscle. One possible explanation for large capacitance values is that the end of an omohyoid fiber might be an anomalous region in which considerable membrane folding occurs, thereby increasing the effective capacitance. It is important to consider such a possibility since the three-microelectrode method is based on the assumption that fiber electrical properties do not vary as the end of the fiber is approached. In frog sartorius muscle fibers, Milton et al. (1982) have questioned the applicability of this assumption and of the three-microelectrode method. As already pointed out, however, the potassium currents we have measured at 20°C in the omohyoid with the three-microelectrode method agree well with those measured by Pappone (1980). Moreover, any conclusion about the applicability of the three-microelectrode voltage clamp to the omohyoid muscle based only on our values for capacitance seems unwarranted given the variability in the values others have reported for capacitance at the center of mammalian muscle. For example, Adrian and Marshall (1977) found mean values of 3.04, 7.03, and 9.4 $\mu F/cm^2$ (in solutions of varying composition or temperature), Duval and Léoty (1978) found a mean value of 6.9, and Pappone (1980) found a mean of 5.87.

Since our method of normalizing the membrane current leads to a value of C_m that depends inversely on $\sqrt{r_i}$, an alternative explanation for the somewhat higher than expected values of C_m reported here is that they result from underestimates of r_i. Such an underestimate could be the result of a leak resistance at the site of impalement by the current-passing electrode: since the intent of our experiments was not the precise measurement of fiber cable properties but rather the measurement of K currents with good temporal resolution, relatively low-resistance current-passing electrodes were used because they greatly improved the speed of the voltage clamp. Support for the idea that a leak at the current electrode increased the calculated magnitude of C_m is provided by the frequent observation of fibers in which both the holding current and the value of C_m gradually increased with time, whereas the space constant (whose value is unaffected by a leak at the site of the current electrode: cf. Eq. 1 of Schneider and Chandler, 1976) remained relatively constant. A leak at the site of the current electrode does not compromise the ability of the three-microelectrode voltage clamp to measure the voltage dependence or kinetics of channel gating.

Because the normalization of current and the normalization of C_m both depend in exactly the same way on r_i, any errors in this normalization will be cancelled if the current is normalized by capacitance (Schneider and Chandler, 1976). For this reason, values of current density or conductance are always presented together with the values of C_m determined in the same fibers.

Possible Contamination by Other Currents

If the total outward current in rat omohyoid muscle were composed of the sum of two or more separate ionic currents, a differential effect of temperature

on these component currents could be responsible for the observed changes in potassium current time course. For example, the slow phase of outward current seen at low temperatures (Fig. 11C) might represent the activation of potassium channels that gate more slowly than ordinary delayed rectifier channels. This suggestion is lent plausibility by reports of the presence of two or more distinct delayed K channels in a variety of preparations (Adrian et al., 1970*b*; Stanfield, 1970; Duval and Léoty, 1980*b*; Dubois, 1981). The question of whether more than one delayed K channel contributes to outward currents in the omohyoid is addressed at length in the next paper (Beam and Donaldson, 1983). The conclusion drawn there is that only a single delayed K channel is present.

Inward calcium currents are another possible contaminant of the outward K current. A calcium current can be measured in isolation in fibers of the omohyoid after K channels have been blocked by the addition of tetraethylammonium ion (Donaldson and Beam, 1982). At temperatures below ~20°C, the calcium current is sufficiently small and slow as to be negligible; as temperature is increased from 20° up to physiological, the size of the current and the speed of its activation increase dramatically (Donaldson and Beam, 1982). Even at physiological temperatures, however, the calcium current is too small and slow to significantly obscure the time course of potassium current activation, although the activation of calcium current may be responsible in part for the gradual decline of outward current during a maintained depolarization. A third source of potential contamination of the outward current is the known nonlinearity of the capacitance of skeletal muscle fibers. This nonlinearity, which would not have been corrected for by the leak subtraction procedure used here, is thought to be due to the presence of a voltage-dependent charge movement (Schneider and Chandler, 1973; but see Mathias et al., 1980). The current carried by this charge in the omohyoid (Simon and Beam, 1982) is sufficiently fast and small that it should not have seriously contaminated the kinetics of either activation or tail current decay.

A final kind of kinetic contamination to be considered is that caused by K accumulation during outward currents. For a 100-ms test step to +10 mV, accumulation produces a depolarizing shift in V_K on the order of 15 mV (Beam and Donaldson, 1983). For a fiber with $V_K = -75$ mV prior to accumulation, this shift corresponds to an 18% decrease in driving force at +10 mV. Hence, for long depolarizing pulses, the measured current yields an underestimate of the real increase in K conductance. Although it seems likely that accumulation does contaminate the kinetics of the slow phase of outward current that is seen in the cold, it seems unlikely that it influences the initial rising phase at any temperature. Nor does it seem likely that accumulation is significantly involved in the temperature-induced qualitative changes in activation kinetics since these changes are all evident on a time scale of ≤25 ms.

K Channel Gating in the Omohyoid Muscle

Because it appears that the delayed outward current in the omohyoid is contributed by a single kind of K channel with little contamination by other

currents, the measured current should be a measure of the gating of this K channel. As already discussed, this gating can be described to a first approximation by the theory of Hodgkin and Huxley (1952). However, important discrepancies exist between their theory and the measured currents. These discrepancies include: (*a*) over a broad range of temperatures the time course of potassium current activation differs qualitatively from n^4 kinetics; (*b*) tail currents decay more slowly than predicted by n^4 kinetics; (*c*) the time course of tail currents differs qualitatively from n^4 kinetics; (*d*) changing temperature causes qualitative changes in activation kinetics.

The failure of n^4 kinetics to completely account for K channel gating is of course not unique to mammalian skeletal muscle. For example, results similar to point *a* have also been reported for frog myelinated nerve and squid giant axon. In the frog, n raised to varying integral values does not describe the currents activated by a depolarizing test pulse which is preceded by a hyperpolarizing conditioning pulse (Palti et al., 1976). In the squid, n^4 kinetics suffice for small depolarizations, but for large ones neither n^4 nor n^x (for x any positive real number) is adequate (Clay and Shlesinger, 1982). A result similar to point *b* above has been described for sodium currents measured in giant axons chemically treated in order to remove inactivation: m^3 kinetics, which adequately describe the time course of activation, predict a rate of tail current decay more rapid than that actually observed (Oxford, 1981).

One alternative to the HH theory is to suppose that a potassium channel must pass through a sequence of kinetically distinct, closed states before opening. In particular, one might suppose that the gating of the K channel in the omohyoid can be described by a scheme of the sort:

$$\begin{array}{ccccc} C_1 & \longleftrightarrow & C_2 & \longleftrightarrow & C_3 \longleftrightarrow O \\ \uparrow\downarrow & & & & \uparrow\downarrow \\ I_C & & & & I_O \end{array} \qquad (11)$$

In this scheme C_1, C_2, and C_3 represent three closed states of the channel, O indicates the open state of the channel, I_C indicates an inactivated state that can be reached only from the C_1 state, and I_O is an inactivated state reached only from the open state. This scheme represents an amalgam of models developed to describe K channels in other preparations. The presence of several closed states is necessary to account for the sigmoidal time course of activation (although three closed states are indicated, the exact number may be different). In addition, sequential schemes can account for hyperpolarization-induced delays in activation (Young and Moore, 1981). Such a delay, frequently termed the Cole-Moore shift, cannot be accounted for by the n^4 formalism and has been described in a variety of preparations including the squid (Cole and Moore, 1960; Moore and Young, 1981; Clay and Shlesinger, 1982), crayfish (Young and Moore, 1981) and *Myxicola* (Schauf et al., 1976) giant axons, and in frog myelinated nerves (Palti et al., 1976; Begenisich, 1979). One could imagine that an interaction between temperature and the Cole-Moore shift mechanism might provide an explanation for the effect of

temperature on K current kinetics in the omohyoid (point *d* above). Specifically, the −90-mV holding potential used in our experiments might have been sufficient to partially activate the Cole-Moore shift. If the degree of Cole-Moore shift differed at different temperatures, changing temperature would be expected to affect activation kinetics. This explanation does not, however, appear to apply to the omohyoid since our preliminary experiments suggest that prepulses of amplitude from −150 to −60 mV and of duration up to 512 ms have no effect on the kinetics of a current activated by an immediately following test pulse.

States equivalent to I_C and I_O were postulated by Aldrich (1981) to account for cumulative and ordinary inactivation in molluscan neurons. Ordinary inactivation of potassium currents occurs in a variety of preparations (see Aldrich, 1981, for references) including rat iliacus, soleus (Duval and Léoty, 1980*b*), and omohyoid muscles (Beam and Donaldson, unpublished observations). Thus, during a long maintained depolarization the potassium current reaches a peak and then gradually declines to a nonzero level. Besides accounting for this ordinary inactivation, Aldrich points out that the existence of an I_O state implies the presence of a slow phase of tail current decay. During a depolarizing conditioning pulse, channels would enter both the O and I_O states; when the cell was repolarized, K conductance would rapidly decrease as channels proceeded from O to C_3, but a slowly declining phase of conductance would also be present as channels in the I_O state returned to the closed states by way of the open state. Conceivably, this mechanism accounts for the slow kinetic phase of tail current decay observed at potentials of about −70 mV and above. If this theory is correct, then a slow kinetic phase should also have been present in tail currents at more hyperpolarized potentials, although perhaps of small amplitude since the lifetime of the open state becomes very much shorter with hyperpolarization. In any case, for inward tail currents, unambiguous identification of a slow kinetic phase arising from an $I_O \rightarrow O$ transition would be made difficult by the presence of a large slow component of inward current that arises from K accumulation (Beam and Donaldson, 1983).

In addition to ordinary inactivation, cumulative inactivation also appears to be present in the omohyoid (Fig. 2). Such cumulative inactivation has been described in detail in molluscan neurons (Aldrich et al., 1979). In both preparations, a dimunition occurs in the outward current in response to identical test pulses sufficiently brief that little or no ordinary inactivation occurs during any individual pulse. The presence of a state like I_C can account for such cumulative inactivation (Aldrich, 1981).

The next step in our analysis will be to determine whether a scheme resembling reaction 11 can account quantitatively for K channel gating in the omohyoid muscle. However, the effects of temperature suggest that a process something like it must be applicable. With a scheme like 11, the qualitative shape of the current's time course depends on the relative magnitudes of the rate constants linking the various states. A differential effect of temperature on these rate constants would therefore produce the observed behavior of

qualitative changes in current time course. In fact, the effects of temperature should be an aid in distinguishing between alternative gating schemes for the K channel. In this regard, mammalian skeletal muscle, with its ability to survive well in vitro over a broad range of temperatures, should prove to be a valuable preparation.

We wish to thank Dr. D. Campbell for helpful discussions and for reading the manuscript. This work was supported by the Muscular Dystrophy Association and NS 14901.

Received for publication 24 May 1982 and in revised form 27 September 1982.

REFERENCES

Adrian, R. H., W. K. Chandler, and A. L. Hodgkin. 1970*a*. Voltage clamp experiments in striated muscle fibers. *J. Physiol.* (*Lond.*). 208:607–644.

Adrian, R. H., W. K. Chandler, and A. L. Hodgkin. 1970*b*. Slow changes in potassium permeability in skeletal muscle. *J. Physiol.* (*Lond.*). 208:645–668.

Adrian R. H., and M. W. Marshall. 1976. Action potentials reconstructed in normal and myotonic muscle fibers. *J. Physiol.* (*Lond.*). 258:125–143.

Adrian, R. H., and M. W. Marshall. 1977. Sodium currents in mammalian muscle. *J. Physiol.* (*Lond.*). 268:223–250.

Aldrich, R. W. 1981. Inactivation of voltage-gated delayed potassium current in molluscan neurons. *Biophys. J.* 36:519–532.

Aldrich, R. W., P. A. Getting, and S. H. Thompson. 1979. Inactivation of delayed outward current in molluscan somata. *J. Physiol.* (*Lond.*). 291:507–530.

Beam, K. G. 1981. Potassium currents in mammalian muscle. *Biophys. J.* 33:72*a*. (Abstr.)

Beam, K. G., and P. L. Donaldson. 1983. Slow components of potassium tail currents in rat skeletal muscle. *J. Gen. Physiol.* 81:513–530.

Bean, B. P., P. Shrager, and D. A. Goldstein. 1981. Modification of sodium and potassium channel gating kinetics by ether and halothane. *J. Gen. Physiol.* 77:233–253.

Begenisich, T. 1979. Conditioning hyperpolarization-induced delays in the potassium channels of myelinated nerve. *Biophys. J.* 27:257–266.

Begenisich, T., and C. F. Stevens. 1975. How many conductance states do potassium channels have? *Biophys. J.* 15:843–846.

Blatz, A. L. 1981. Low external pH blocks and shifts K channel of frog skeletal muscle. *Biophys. J.* 33:70*a*. (Abstr.)

Brismar, T. 1980. Potential clamp analysis of membrane currents in rat myelinated nerve fibers. *J. Physiol.* (*Lond.*). 298:171–184.

Camerino, D., and S. H. Bryant. 1976. Effects of denervation and colchicine treatment on the chloride conductance of rat skeletal muscle fibers. *J. Neurobiol.* 7:221–228.

Chiu, S. Y., H. E. Mrose, and J. M. Ritchie. 1979*a*. Anomalous temperature dependence of the sodium conductance in rabbit nerve compared with frog nerve. *Nature* (*Lond.*). 279:327–328.

Chiu, S. Y., J. M. Ritchie, R. B. Rogart, and D. Stagg. 1979*b*. A quantitative description of membrane currents in rabbit myelinated nerve. *J. Physiol.* (*Lond.*). 292:149–166.

Clay, J. R., and M. F. Shlesinger. 1982. Delayed kinetics of squid axon potassium channels do not always superimpose after time translation. *Biophys. J.* 37:677–680.

Cole, K. S., and J. W. Moore. 1960. Potassium ion current in the squid giant axon: dynamic characteristic. *Biophys. J.* 1:1–14.

Costantin, L. L. 1968. The effect of calcium on contraction and conductance thresholds in frog skeletal muscle. *J. Physiol. (Lond.)*. 195:119–132.

Donaldson, P. L., and K. G. Beam. 1982. Calcium currents in mammalian skeletal muscle. *Biophys. J.* 37:340*a*. (Abstr.)

Dreyer, F., K.-D. Müller, K. Peper, and R. Sterz. 1976. The *M. omohyoideus* of the mouse as a convenient mammalian muscle preparation. A study of junctional and extrajunctional acetylcholine receptors by noise analysis and cooperativity. *Pflügers Arch. Eur. J. Physiol.* 367:115–122.

Dubois, J. M. 1981. Evidence for the existence of three types of potassium channels in the frog Ranvier node membrane. *J. Physiol. (Lond.)*. 318:297–316.

Duval, A., and C. Léoty. 1978. Ionic currents in mammalian fast skeletal muscle. *J. Physiol. (Lond.)*. 278:403–423.

Duval, A., and C. Léoty. 1980*a*. Ionic currents in slow twitch skeletal muscle in the rat. *J. Physiol. (Lond.)*. 307:23–41.

Duval, A., and C. Léoty. 1980*b*. Comparison between the delayed outward current in slow and fast twitch skeletal muscles in the rat. *J. Physiol. (Lond.)*. 307:43–57.

Haydon, D. A., and J. E. Kimura. 1981. Some effects of *n*-pentane on the sodium and potassium currents of the squid giant axon. *J. Physiol. (Lond.)*. 312:57–70.

Hodgkin, A. L., and A. F. Huxley. 1952. A quantitative description of membrane current and its application to conduction and excitation in nerve. *J. Physiol. (Lond.)*. 117:500–544.

Hodgkin, A. L., and S. Nakajima. 1972. The effect of diameter on the electrical constants of frog skeletal muscle fibers. *J. Physiol. (Lond.)*. 221:105–120.

Kukita, F. 1982. Properties of sodium and potassium channels of the squid giant axon far below 0°C. *J. Membr. Biol.* 68:151–160.

Lass, Y., and G. D. Fischbach. 1976. A discontinuous relationship between the acetylcholine-activated channel conductance and temperature. *Nature (Lond.)*. 263:150–151.

Mathias, R. T., R. A. Levis, and R. S. Eisenberg. 1980. Electrical models of excitation contraction coupling and charge movement in skeletal muscle. *J. Gen. Physiol.* 76:1–31.

Milton, R. J., R. T. Mathias, and R. S. Eisenberg. 1982. Impedance measurements at the pelvic end of frog sartorius muscle fibers. *Biophys. J.* 37:356*a*. (Abstr.)

Moore, J. W., and S. H. Young. 1981. Dynamics of potassium ion currents in squid giant axon membrane. A reexamination. *Biophys. J.* 36:715–722.

Müntener, M., J. Gottschall, W. Neuhuber, A. Mysicka, and W. Zenker. 1980. The ansa cervicalis and the infrahyoid muscles of the rat. *Anat. Embryol.* 159:49–57.

Oxford, G. S. 1981. Some kinetic and steady-state properties of sodium channels after removal of inactivation. *J. Gen. Physiol.* 77:1–22.

Palade, P. T., and R. L. Barchi. 1977. Characteristics of the chloride conductance in muscle fibers of the rat diaphragm. *J. Gen. Physiol.* 69:325–342.

Palade, P. T., and R. L. Barchi. 1977. Characteristics of the chloride conductance in muscle fibers of the rat diaphragm. *J. Gen. Physiol.* 69:325–342.

Palti, Y., G. Ganot, and R. Stämpfli. 1976. Effect of conditioning potential on potassium current kinetics in the frog node. *Biophys. J.* 16:261–273.

Schauf, C. L., T. L. Pencek, and F. A. Davis. 1976. Potassium current kinetics in *Myxicola* axons. *J. Gen. Physiol.* 68:397–403.

Schneider, M. F., and W. K. Chandler. 1973. Voltage dependent charge movement in skeletal muscle: a possible step in excitation contraction coupling. *Nature (Lond.)*. 242:244–246.

Schneider, M. F., and W. K. Chandler. 1976. Effects of membrane potential on the capacitance of skeletal muscle fibers. *J. Gen. Physiol.* 67:125–163.

Simon, B., and K. G. Beam. 1982. Kinetics of voltage-dependent charge movement in mammalian skeletal muscle. *Biophys. J.* 37:24*a*. (Abstr.)

Stanfield, P. R. 1970. The effect of the tetraethylammonium ion on the delayed currents of frog skeletal muscle. *J. Physiol. (Lond.)*. 209:209–229.

Waltman, B. 1966. Electrical properties and fine structure of the ampullary canals of Lorenzini. *Acta Physiol. Scand.* 66(Suppl.):264.

Weast, R. C. 1971. Handbook of Chemistry and Physics. 52nd ed. R. C. Weast, editor. The Chemical Rubber Co., Cleveland. D123.

Woodhull, A. M. 1973. Ionic blockage of sodium channels in nerve. *J. Gen. Physiol.* 61:687–708.

Young, S. H., and J. W. Moore. 1981. Potassium ion currents in the crayfish giant axon. Dynamic characteristics. *Biophys. J.* 36:723–733.